J Therm Anal Calorim (2015) 122:135–144
DOI 10.1007/s10973-015-4718-6

Ammonium alcohol polyvinyl phosphate intercalated LDHs/epoxy nanocomposites

Flame retardancy and mechanical properties

Yanmao Dong[1,2,3] · Yugang Zhu[1] · Xu Dai[1] · Dan Zhao[1] · Xing Zhou[1] · Yu Qi[1] · Joseph H. Koo[3]

Received: 18 July 2014 / Accepted: 19 April 2015 / Published online: 26 May 2015

Abstract To improve the flame retardancy and mechanical properties of epoxy (EP), a novel intercalated layered double hydroxides (ILDHs) were synthesized by a solution intercalation method using ammonium alcohol polyvinyl phosphate as intercalator. The ILDHs were examined by X-ray diffraction, Fourier transform infrared spectroscopy (FTIR), energy-dispersive spectrometry and scanning electron microscopy (SEM). The conditions for synthesis of ILDHs have been optimized. Thermogravimetric analysis indicated a good char-forming property of ILDHs. The flame retardancy of epoxy was improved by adding ILDHs. The EP composites containing 30–40 mass% ILDHs passed UL-94V-0 rating. Tensile strength was also enhanced by adding 30–40 mass% ILDHs, which was attributed to the involvement of physical cross-linking network among layered particles and polymer chains. The morphology and structures of residues generated during LOI test were investigated by SEM and FTIR to support a fundamental analysis for the mechanism of char formation. SEM observations of residues of the ILDHs/EP confirmed the formation of an incompact charred layer during combustion, which could inhibit the transmission of heat and mass during combustion. It may be inferred that ILDHs acted as a catalyst for esterification, dehydration and compact char formation of EP system.

Keywords Flame retardant · Epoxy resin · Ammonium alcohol polyvinyl phosphate · Intercalation · Layered double hydroxides

✉ Yanmao Dong
dongyanmao0512@gmail.com; dongyanmao@163.com

[1] School of Chemistry, Biology and Materials Engineering, Suzhou University of Science and Technology, 1 Kerui Road, Suzhou 215009, JS, China

[2] Jiangsu Key Laboratory for Environment Functional Materials, 1 Kerui Road, Suzhou 215009, JS, China

[3] Department of Mechanical Engineering, The University of Texas at Austin, 204 E. Dean Keaton St.-C2200, Austin, TX 78712, USA

Introduction

Epoxy (EP) resins have been applied in many fields of material, owing to their excellent properties, such as high thermal and mechanical stability along with good chemical resistance. However, epoxy resins usually perform poorly under fire, burning easily and violently. So, many nano-sized flame retardants have to be employed to protect EP, such as clay and layered double hydroxides (LDHs) [1]. The flammability performance of these polymer nanocomposites has been studied extensively. By adding LDHs, the rate of char formation at low temperature was increased and the thermal stability was enhanced at high temperature [2]. LDHs also acted as a heat stabilizer and efficient smoke suppressant, which is attributed to the better dispersion of LDHs in the bulk phase of resin [3]. The mechanism of fire retardancy on the epoxy by these LDHs is the formation of carbonaceous char, which is a barrier to the heat and mass transfer that occurs during combustion of polymer nanocomposites [4]. However, LDHs show strong interactions between the nanolayers, making it difficult to exfoliate them when mixing with polymers. To enhance the compatibility and flame retardancy, LDHs modified by intercalation have been studied extensively. The Mg–Al LDHs have modified by different intercalating agents, such as dodecyl sulfate [5], glycinate [6], poly(oxypropylene)-amindocarboxylic acid (POP-

amido acid) [7], amino benzoate and carbonate [8], and amino laurate [9]. The effects of the addition of these modified LDHs on the mechanical, thermal and fire retardancy properties of polymer nanocomposites have been investigated. The enhanced performance of the epoxy/LDHs nanocomposites could be attributed to the better dispersion state of the LDHs layers in the EP matrix and the greater diffusion-hindering effect of LDHs layers on oxygen and volatile products throughout the composite materials when they were exposed to thermal degradation. As a polar polymer, PVA has been modified by LDHs to promote the thermal, morphological and mechanical properties via the interaction between the PVA and the LDHs by hydrogen bonding through hydroxyl groups [10–12]. PVA also showed good compatibility with ammonium dihydrogen phosphate ($NH_4H_2PO_4$, ADP) [13] and synergistic flame retardancy with ammonium polyphosphate (APP)/LDHs [14]. Because of the reaction between the amine groups of the intercalated amino compound and the epoxy groups, the adhesion between the LDHs nanolayers and epoxy molecules makes these LDHs/epoxy nanocomposites more compatible. Consequently, the tensile and the mechanical properties of polymer nanocomposites were also enhanced.

The focus of the present work is to synthesize Mg/Al LDHs intercalated by ammonium alcohol polyvinyl phosphate (AAPP). The mechanical, thermal and flame-retardant properties of the intercalated LDHs (ILDHs) have been evaluated. The mechanical properties were investigated with tensile testing. The flame-retardant characteristics were evaluated by limiting oxygen index (LOI) and vertical burning (UL 94), and the burnt sample residues were examined by scanning electron microscopy and Fourier transform infrared spectroscopy.

Experimental

Materials

$MgCl_2{\cdot}6H_2O$ was supplied by Tongya Chemical Science and Technology Development Corp (Shanghai, China). $Al_2(SO_4)_3{\cdot}18H_2O$ was obtained from Tianjin Damao Chemical Reagent Corp (Tianjin, China). Sodium hydroxide was purchased from Shanghai Chemical Reagent Corp (Shanghai, China). Na_2CO_3 was acquired from Nanjing Chemical Reagent Corp (Nanjing, China). H_3PO_4 was supplied by Shanghai Lianshi Chemical Reagent Corp (Shanghai, China). Urea was obtained from Shanghai No. 1 Chemical Reagent Corp (Shanghai, China). Epoxy (E-44), a bisphenol A type epoxy resin with low molecular weight, was supplied by Zhenjiang Danbao Resin Corp (Zhenjiang, China). Ethylenediamine was acquired from Shanghai Qiangshun Chemical Industry Corp (Shanghai, China). Poly (vinyl alcohol) ($M_n = 75{,}000$ g mol^{-1}) having a saponification degree of 99 mol% or more (PVA-1799) used in this work was provided by Shanghai Shanpu Chemical Industry Corp (Shanghai, China). Commercial Mg–Al layered double hydroxides (LDHs-0) were purchased from Nantong Advance Chemicals Co., Ltd.

Preparation of AAPP

The AAPP was synthesized according to the literature [15]. The typical synthetic steps of AAPP are listed as follows: Firstly, the PVA was dissolved in deionized water in a beaker to obtain the PVA aqueous solution A. Secondly, the aqueous solution B was obtained by blending and heating the phosphoric acid (85 %) with urea (at 85 °C for 2 h) in a three-necked bottle. Thirdly, the solution A was added to solution B in 3 equal batches, combining with stirring and refluxing for 2 h. After reaction, the solution was cooled and precipitated in a 95 % ethanol aqueous solution. The product obtained by suction filter was washed until the aqueous solution was neutral. Finally, the AAPP was acquired by vacuum drying of the wet product under 60 °C for 24 h.

Preparation of AAPP intercalated layered double hydroxides

The AAPP intercalated layered double hydroxides (ILDHs) were prepared using the co-precipitation method. The AAPP was dissolved in 100 mL of deionized water in a three-necked bottle to obtain solution A. $MgCl_2$ 12.18 g (0.06 mol) and $Al_2(SO_4)_3$ 6.66 g (0.01 mol) were dissolved in 50 mL of deionized water to obtain solution B. NaOH 6.4 g (0.16 mol) and Na_2CO_3 1.06 g (0.01 mol) were dissolved in 50 mL of deionized water to obtain solution C. The mixed solution B and solution C were then slowly added in solution A with vigorous stirring for a certain time (from 0.5 to 4 h). During processing, a sonication was used to disperse the ILDHs at room temperature. After reaction, the obtained slurry was filtered to obtain the raw product, followed by washing several times using the dispersion and filtration processes in distilled water and then drying at 105 °C for 6 h.

The different ILDHs used in this study were synthesized almost in the same way, just with little differences in APP-to-LDHs mole ratio (1:4–5:4), reaction time (0.5–4 h) and reaction temperature (60–100 °C). Composition of the reactants, reaction conditions and nomenclature are listed in Table 1. The pure Mg–Al LDHs (LDHs-1) were also prepared for study.

Table 1 Composition of the reactants, reaction conditions and nomenclature

Nomenclature	AAPP-to-LDHs mole ratio	Reaction time/h	Reaction temperature/°C
ILDHs-1-1	1:4	2	80
ILDHs-1-2	1:2	2	80
ILDHs-1-3	3:4	2	80
ILDHs-1-4	1:1	2	80
ILDHs-1-5	5:4	2	80
ILDHs-2-1	1:2	0.5	80
ILDHs-2-2	1:2	1	80
ILDHs-2-3	1:2	2	80
ILDHs-2-4	1:2	3	80
ILDHs-2-5	1:2	4	80
ILDHs-3-1	1:2	2	60
ILDHs-3-2	1:2	2	70
ILDHs-3-3	1:2	2	80
ILDHs-3-4	1:2	2	90
ILDHs-3-5	1:2	2	100

Preparation of ILDHs/EP composites

ILDHs-1-2 2.75 g and EP 10 g were blended uniformly under ultrasonic condition, and then, ethylenediamine anhydrous was dispersed in the solution above to prepare the ILDHs-1-2/EP composite. After ambient cure for 24 h, the ILDHs-1-2/EP was cured for 2 h at 120 °C. The ILDHs-1-2/EP samples containing 5 mass% ILDHs-1-2 (ILDHs/EP-5) were obtained. Using this method, other ILDHs-1-2/EP samples containing 10 mass% (ILDHs/EP-10), 20 mass% (ILDHs/EP-20), 30 mass% (ILDHs/EP-30) and 40 mass% (ILDHs/EP-40) ILDHs-1-2 were also prepared.

Characterization and measurement

X-ray diffraction (XRD) profiles were carried out on a D8 focus electronic instrument in steps of 6° min^{-1} using Cu K_α radiation ($\lambda = 0.15418$ nm) at 45 kV and 150 mA between 5° and 70° (2θ).

The limiting oxygen index (LOI) values were measured on an HC900-2 oxygen index meter (Jiangning, China). The specimens used for the test were prepared by molding method according to GB/T10801.1-2002.

UL-94, a standard, small-scale flame test for flammability of plastic materials, determines the material's tendency to either self-extinguish or spread its flame once the specimen has been ignited. Ratings for UL-94 range from V-2 to V-0. V-0 is the best rating for a polymer that self-extinguishes, and also the polymer does not drip flaming fragments. Materials were tested as received with no additional conditioning before testing. Five specimens for each formulation were tested. The UL-94 tests were performed on a CFZ 2-type instrument (Jiangning, China).

Mechanical properties of epoxy nanocomposites were evaluated using an XLD-1A universal material testing system (Tianjin, China) in accordance with GB/T 1093-92 test for plastics. The load–displacement curve was obtained, and the ultimate tensile stress (UTS) and elongation at break were calculated accordingly. Average values were reported based on five samples that were tested for each formulation. The specimens were conditioned at 50 % relative humidity for 48 h before testing. The testing rate was 10 mm min^{-1}, and the environmental temperature was 23 °C.

Thermogravimetric (TG) analysis and differential thermogravimetric (DTG) analysis on EP composites (approximately 8.0 mg) were characterized on a DTG-60 instrument in flowing air at 10 °C min^{-1} from room temperature to 700 °C.

Fourier transform infrared (FTIR) studies were recorded on a Nicolet Magna-IR 550 spectrometer. The sample prepared in this paper was pressed pellet of sample combined with KBr.

Morphology analysis of the residues of ILDHs/EP composite after the LOI test was conducted by scanning electron microscopy (SEM) (S-4700 instrument) operating at an accelerating voltage of 20 kV. The associated elemental composition was determined by energy-dispersive analysis by X-ray (EDAX) facility.

Results and discussion

Characterization of ILDHs

The Mg–Al layered double hydroxides (LDHs, $[Mg_6Al_2(-OH)_{16}CO_3]4H_2O$) and AAPP intercalated LDHs (ILDHs) were prepared by chemical co-precipitation method [16] (Fig. 1). These products and commercial Mg–Al LDHs (LDHs-0) were tested by XRD. The powder XRD patterns of the sample are shown in Fig. 2. LDHs layers may exhibit two stacking sequences, rhombohedral and hexagonal. As shown in Fig. 2, the typical diffraction peaks at (003), 006), (009), (015), (018), (110) and (113) belong to LDHs (JCPDS22-0700) [17]. The LDHs are a mixture of hydroxide and carbonate. Some OH-, Cl^-, CO_3^{2-} and SO_4^{2-} exist in the LDHs. The LDHs and ILDHs-1-2 as prepared have the same crystal form. Compared to the XRD patterns of the commercial LDHs, LDHs-1 and ILDHs-1-2 show a broad diffraction peak with an obvious blue shift.

Based on the XRD patterns and the full width at half maximum (FWHM) of the (003), (006) and (009) reflections, the crystallographic data and crystallite size of samples were calculated using the Bragg's law and

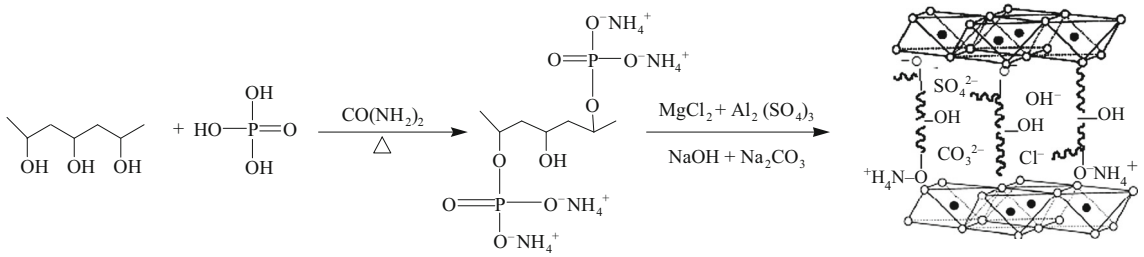

Fig. 1 Schematic diagram of the synthesis of ILDHs

Table 2 Crystallographic data and crystallite size of samples

Sample name	d_{003}/nm	d_{006}/nm	d_{009}/nm	Crystallite size/nm
LDHs-0	0.756	0.380	0.259	–
LDHs-1	0.782	0.393	0.258	6.86
ILDHs-1-2	0.921	0.399	0.262	7.36

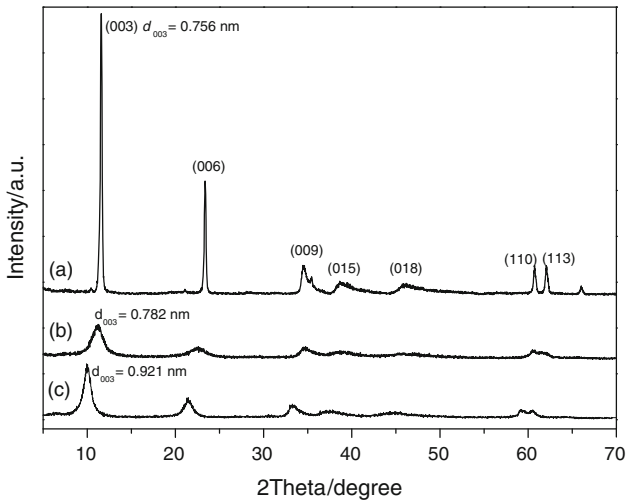

Fig. 2 XRD patterns of **a** LDHs-0, **b** LDHs-1 and **c** ILDHs-1-2

Scherrer's equation [18], respectively. Results are listed in Table 2. Comparing the d_{003}, the d-spacing of LDH-1 and ILDHs-1-2 are greater than that of LDH-0. The interlamellar spacing of ILDHs-1-2 ($d_{003} = 0.921$ nm) is larger than that of LDHs-1 ($d_{003} = 0.782$ nm). The change in interlayer spacing indicates the successful intercalation of LDHs by AAPP [19]. The average thickness of the LDHs-1 and ILDHs crystals is 6.86 nm and 7.36 nm, respectively. Since the d_{003} basal spacing of LDHs-1 and ILDH is 0.782 nm and 0.921 nm, respectively, the thickness value suggests that the obtained crystallites contain stacks of up to 8–10 LDH layers.

The intercalation of AAPP into LDHs was also confirmed by the FTIR spectra (Fig. 3). The spectrum of AAPP sample (Fig. 3a) shows –NH (3419 and 1409 cm^{-1}),

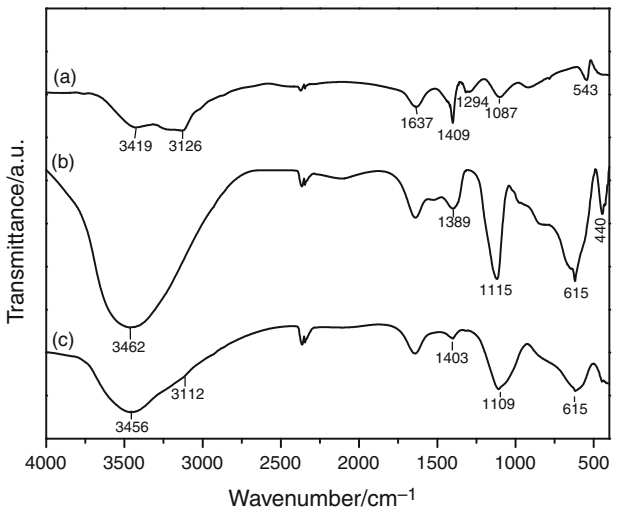

Fig. 3 FTIR patterns of **a** AAPP, **b** LDHs-1 and **c** ILDHs-1-2

–OH (3126 cm^{-1}, hydrate complex), –C=O (1637 cm^{-1}), C–O–P (1294 and 543 cm^{-1}) and P–O (1087 cm^{-1}) groups [17], indicating the presence of carbonate in the sample. The spectrum of LDHs-0 sample (Fig. 3b) shows the characteristic peaks of the LDHs materials: (1) the intense broad band around 3300–3500 cm^{-1} (center at 3462 cm^{-1}) associated with the stretching vibration of O–H in the brucite-like layer and water molecules;(2) bands around 1389 and 1115 cm^{-1} are attributed to the asymmetric and symmetric stretching vibrations of carboxylate, respectively, indicating the presence of carbonate in the sample; (3) the band at 615 cm^{-1} attributed to the M–O and M–O–H stretching vibrations; and (4) the peak at 440 cm^{-1}, particularly characteristic of Mg–Al–LDH materials. Figure 3c presents the FTIR spectrum of ILDHs-1-2, which contains some carbonate and hydroxide. The asymmetric carboxylate band moved to a lower frequency compared with the corresponding bands in AAPP, due to the strong electrostatic interactions between AAPP –OH and $–NH_4^+$ groups and LDHs layers. For example, 3126 and 1409 cm^{-1} of AAPP and 1115 cm^{-1} of LDHs shift to 3112, 1403 and 1109 cm^{-1}, respectively, after intercalation

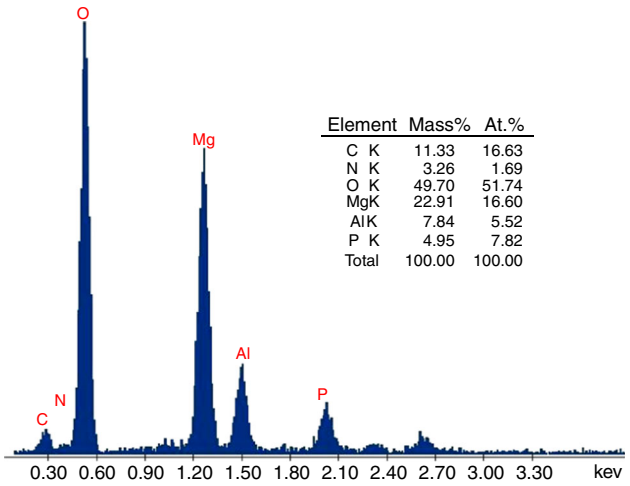

Fig. 4 EDAX pattern and elemental composition (*inset* table) of ILDHs-1-2

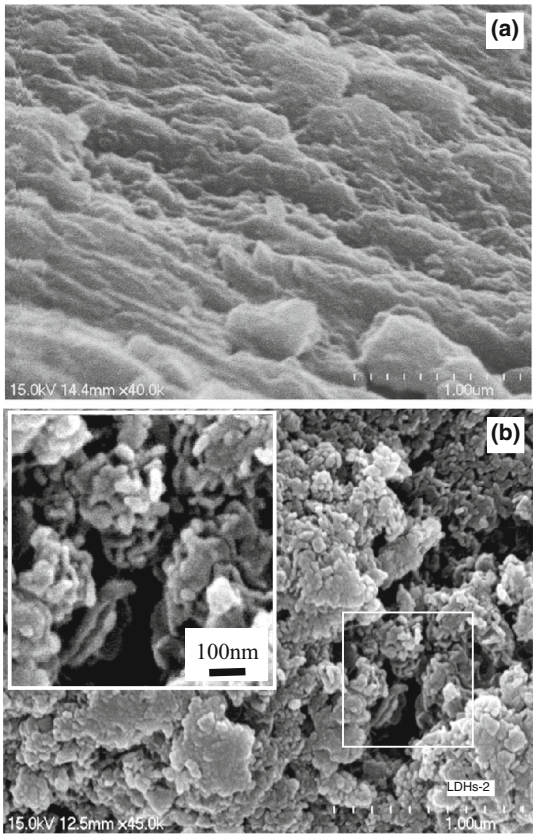

Fig. 5 SEM micrograph of **a** LDHs-1 and **b** ILDHs-1-2

to LDHs. The FTIR analysis shows good interaction between the AAPP and the LDHs [20, 21].

Figure 4 presents the EDS pattern and elemental composition (inset) of ILDHs. Results illuminate that the Mg-to-Al mole ratio is about 3:1, which is the same as the theoretical result of LDHs. In addition, the content of N and P elements in the ILDHs is 1.69 AT % and 7.82 AT %, respectively, which confirms the intercalation of the LDHs by AAPP.

Figure 5 presents the morphology of LDHs and ILDHs as revealed by SEM. The aggregation of LDHs-1 (Fig. 5a) with relative flat surface is observed. In comparison with the LDHs-1, the ILDHs-1-2 (Fig. 5b) accumulates layer by layer to form the laminate structure with rough and porous surface, resulting in a huge specific surface area and pore volume. The inset shows the detail morphology of ILDHs-1-2. The thickness of laminate structure is about 30–40 nm, which is larger than that calculated from the XRD patterns using Scherrer's formula (6.86–7.36 nm). The difference may be due to some aggregation of the ILDHs nanocrystals. The data calculated from XRD results reflected the size of a single crystal, whereas the SEM photograph shows the aggregates of the ILDHs particles. Due to their porous surface and nano-sized laminate structure, the ILDHs indicate a good compatibility with polymers. Based on the analysis by XRD and SEM, it can be concluded that AAPP has been intercalated into the LDHs layers [16].

Impact factors for the synthesis of ILDHs

The effects of AAPP-to-LDHs ratio, reaction time and reaction time on the yield of ILDHs have been studied. As shown in Table 3, the yield of ILDHs increases from 63.6 to 74.0 % with the increase in AAPP-to-LDHs mole ratio from 1:4 to 1:1, and then, the yield decreases as the mole ratio reaches 5:4. The maximum yield of ILDHs was obtained as the reaction time was 2 h. Results show that the yield of ILDHs increases from 68.6 to 71.1 % as the reaction temperature increases from 60 to 100 °C. Based on the analysis aforementioned, the optimized conditions for synthesis of ILDHs are as follows: an AAPP-to-LDHs ratio of 1:2–1:1, a reaction time of 2–3 h and a reaction time of ~90 °C.

Table 3 Effects of AAPP-to-LDHs ratio, reaction time and reaction temperature on the yield of ILDHs

Sample	Yield/%	Sample	Yield/%	Sample	Yield/%
ILDHs-1-1	63.6	ILDHs-2-1	59	ILDHs-3-1	68.6
ILDHs-1-2	72.5	ILDHs-2-2	66.2	ILDHs-3-2	69.7
ILDHs-1-3	73.3	ILDHs-2-3	73.6	ILDHs-3-3	70.2
ILDHs-1-4	74.0	ILDHs-2-4	72.9	ILDHs-3-4	70.9
ILDHs-1-5	73	ILDHs-2-5	73	ILDHs-3-5	71.1

Mechanical properties

The mechanical properties of epoxy nanocomposites were evaluated, and the ultimate tensile stress (UTS) and

Table 4 Mechanical properties of EP, LDHs/EP and ILDHs/EP

Sample	Tensile strength/MPa	Elongation at break/%
EP	41.98 ± 1.6	58 ± 1.6
LDHs-1/EP	26.35 ± 1.4	30 ± 1.8
ILDHs/EP-10	43.40 ± 2.6	32 ± 1.9
ILDHs/EP-20	52.53 ± 1.9	35 ± 2.1
ILDHs/EP-30	29.67 ± 1.8	33 ± 1.7
ILDHs/EP-40	20.86 ± 2.2	29 ± 1.5

elongation at break were calculated accordingly. Table 4 illustrates the mechanical properties of neat EP, LDHs-1/EP and ILDHs-1-2/EP samples. According to the experimental data, the addition of LDHs-1 reduces mechanical properties of EP [5]. The reduction in tensile strength and elongation at break is of 37 and 47 %, respectively. However, results show that some mechanical properties of ILDHs-1-2/EP composite (ILDHs/EP-10 and ILDHs/EP-20) are significantly improved compared to the LDHs-1/EP and neat epoxy samples. For example, by adding 20 mass% ILDHs-1-2, the tensile strength of ILDHs/EP-20 increases 25 and 99 % in comparison with the neat epoxy and LDHs-1/EP, respectively. The elongation at break of ILDHs/EP-20 is higher than that of LDHs-1/EP, but ILDHs/EP-40 is less than that of neat epoxy [22].

It suggests that there exists a physical cross-linking network composed of layered particles and polymer chains in the composites (Fig. 6) [23]. As the schematic diagram of cross-linking network of ILDHs/EP shows (Fig. 6), the transformation and movement of ILDHs and EP occur simultaneously. The ILDHs with hydrophobic property easily disperse in epoxy resin, and the ILDHs with large gallery space allow the epoxy molecules and the curing agents to easily diffuse into the LDHs galleries at elevated temperature. Owing to the physical interaction and chemical reaction between the amine groups of the intercalated amino and epoxy groups, the adhesion between the LDHs nanolayers and epoxy molecules makes these LDHs/epoxy nanocomposites more compatible. Consequently, the tensile properties from tensile test and the mechanical properties were enhanced [8, 9]. As the ILDHs loading goes over 20 mass%, the stress concentration resulting from agglomeration of ILDHs decreases the mechanical properties of ILDHs/EP [24].

Thermal properties

The thermal stability of epoxy composites is extremely important when it comes to flame retardancy, which are mainly evaluated by their release of decomposition products and formation of char. Figure 7a shows TG data of

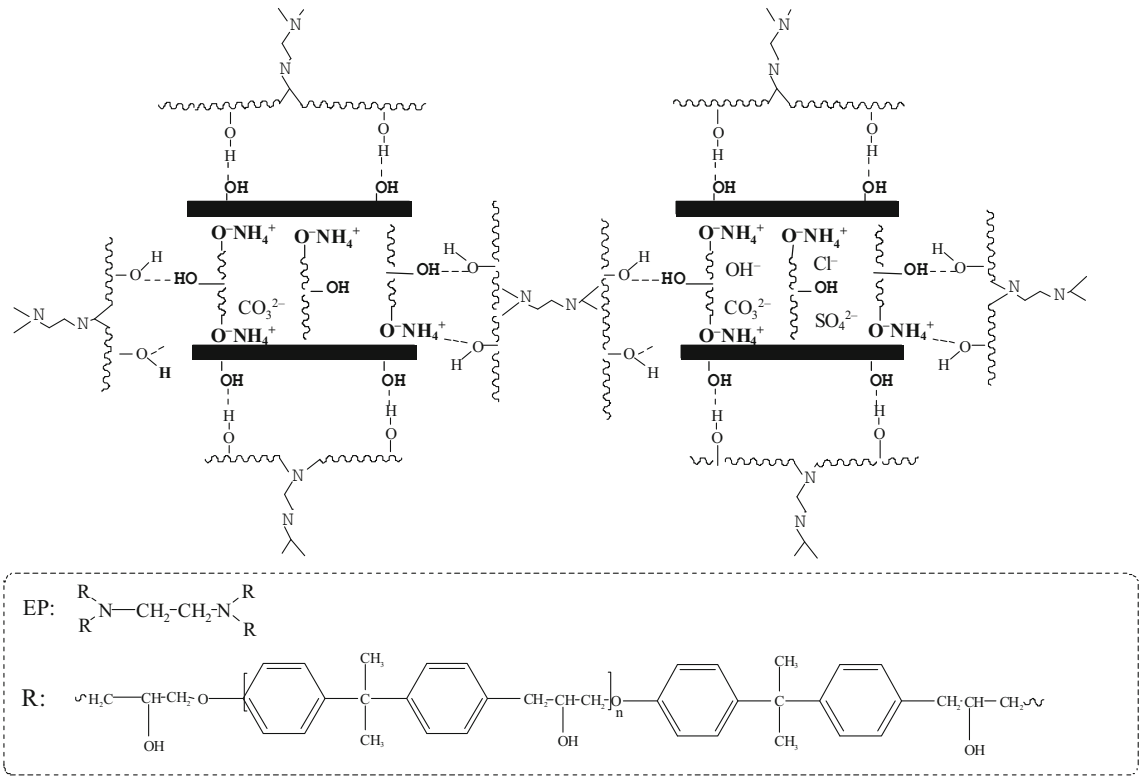

Fig. 6 Schematic diagram of cross-linking network of ILDHs/EP

LDHs-1, EP and ILDHs-1-2 samples in air. DTG curves for all samples under air are illustrated in Fig. 7b. It can be seen that the thermal decompositions of LDHs-1 occur at 263 and ~443 °C, indicating the releasing of water and CO_2 [25]. For ILDHs-1-2, the first elimination of H_2O and volatiles occurs in the range of 100–300 °C (~9.41 mass%). The second mass loss occurs at ~451 °C caused by the random scission of molecular main chain of AAPP. The initial thermal decomposition temperature of EP occurs at ~349 °C, which is near to ILDHs-1-2, indicating a good matching of flame retardancy between ILDHs and EP. At ~349 °C, EP decomposed sharply. The thermal decomposition of LDHs leads to the formation of an intercalated nanostructure of the char and mixed metal oxides (Al_2O_3 and $MgAl_2O_4$). The intercalated nanostructure can improve the antioxidation property of the char structure [26, 27].

The TG/DTG curves of EP and ILDHs/EP are shown in Fig. 8. As the ILDHs loading increases from 10 to 40 mass%, the residue mass percent of ILDHs/EP increases from 1 to 30.15 mass%, indicating that catalysis of the ILDHs accelerates the de-polycondensation reaction [28]. In comparison with LDHs/EP, the residue mass percent of ILDHs/EP-20 (18.86 mass%) is higher than that of LDHs/EP-20 (12.13 mass%). Zhao et al. [14] reported the use of APP, and synergistic co-additives such as Ni/Al LDHs can impart good flame retardancy for PVA rather than employing APP alone because LDHs can catalyze esterification, dehydration and compact char formation of PVA/APP system. The improvement in flame retardancy of PVA/APP/LDHs composite was due to condensed-phase flame-retardant mechanism. In my present work, the residue in the TG was evident that ILDHs efficiently promoted the formation of charred layers with phosphocarbonaceous structures; i.e., the synergistic effect between LDHs and

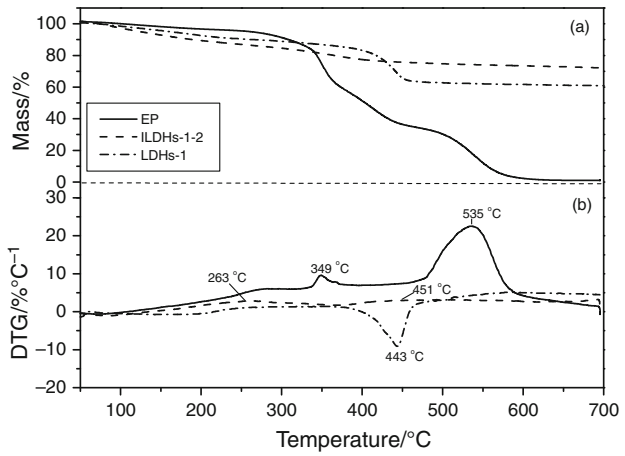

Fig. 7 TG (**a**) and DTG (**b**) curves of LDHs-1, ILDHs-1-2 and EP

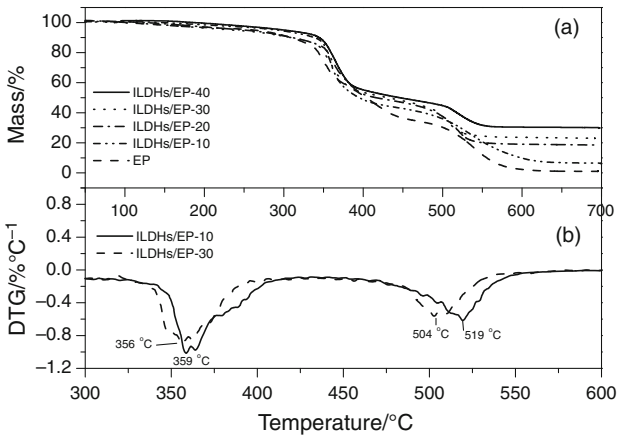

Fig. 8 TG (**a**) and DTG (**b**) curves of EP and ILDHs/EP

AAPP is observed. It is similar with the results of the literature [29].

As shown in DTG curves, the marked peaks of LDHs/EP-1 curve are at 359 and 519 °C, showing a right shift at low temperature and a left shift at high temperature in comparison with EP (Figs. 7, 8). The LDHs/EP-30 shows a similar trend, compared to the EP and LDHs/EP-10 (359 °C → 356 °C; 519 °C → 504 °C), indicating a better stability than that of EP and LDHs/EP-1 at the first decomposition. In summary, ILDHs/EP with a low flammability can effectively inhibit combustion by the major action of condensed-phase protection [23]. The fundamental flame-retardant mechanism will be discussed adequately by the following morphology characterization and FTIR measurements of char layer.

Flammability

Limiting oxygen index (LOI) and vertical burning (UL-94) tests are used as qualitative methods to evaluate the flame retardancy of polymeric materials. All LOI data of ILDHs/EP composites are shown in Table 5. From the experimental data shown in Table 5, pure EP is easily flammable with an LOI value of 19.2 %, and it cannot pass the UL 94 test. The LOI data of LDHs-1/EP (20 mass% LDHs) increase to 22.3 %; however, it cannot achieve a V-0 rating. Obviously as can be seen from Table 5, the flame retardancy of ILDHs/EP composite can be improved effectively with a specific loading of ILDHs. The LOI value of ILDHs/EP-10 is 23.2 %. As the concentration of ILDHs increases from 20 to 40 mass%, the LOI values increase dramatically. The LOI value of ILDHs/EP-40 can reach up to 29.0 %, and UL 94 of ILDHs/EP-30 and ILDHs/EP-40 are rated V-0. All the results above demonstrate that ILDHs play an important role in enhancing flame retardancy of EP composites. This may be due to the reason that as ILDHs/

Table 5 Evaluation of flame retardancy of ILDHs/EP systems

Samples	Loading/mass%	LOI/%	UL-94 rating
EP	0	19.2	N.R
LDHs-1/EP	20	22.3	V-2
ILDHs/EP-10	10	23.2	V-1
ILDHs/EP-20	20	26.1	V-1
ILDHs/EP-30	30	27.4	V-0
ILDHs/EP-40	40	29.0	V-0

EP systems are exposed to fire, a compact and intumescent charred layer on the surface of the composite is formed. This charred layer provides an efficient shield and insulation which can prevent the underlying material from coming into contact with heat, oxygen and fire directly [4]. However, the charred layer of ILDHs/EP system formed during combustion is porous but not compact, which can be seen during LOI test. The structure and formation of the char layer will be discussed in detail below.

Possible mechanism for char formation

To determine how the ILDHs affect the formation of an intumescent charred layer, FTIR spectroscopy was employed to analyze the composition of charred layer of ILDHs/EP-20. The chars were collected after heating at 500 °C for 5 min in air using a muffle furnace. As shown in Fig. 9a, organic groups exist in EP, which are characterized by peaks at 2900, 1567 and 1088 cm^{-1}, etc. This can be attributed to absorption from CH_2 or CH_3 asymmetric–symmetric vibration and deformation vibration. After combustion, as shown in Fig. 9b, the intensity of some peaks at 1639, 990 and 487 cm^{-1} increases significantly with the loading of ILDHs in EP composite. The characteristic absorption peaks at 1198 cm^{-1} (assigned to P=O stretching) and 990 cm^{-1} (attributed to P–O group) become stronger and clearer when compared to Fig. 5a, to some degree [30]. This may be due to the cross-linking of AAPP and EP in the presence of LDHs. So, more AAPP becomes available for phosphorylation and char formation [31]. Furthermore, the broad shoulder peak at ~765 cm^{-1} belongs to the stretching of aromatic structure in the phosphate–carbon complexes. Meanwhile, the vibration of C=C group at 1567 cm^{-1} disappears. Comparing the data with TG graphs (Fig. 8), the residue mass of ILDHs/EP-20 (18.86 mass%) is higher than that of LDHs/EP-20 (12.13 mass%), indicating that the phosphocarbonaceous complexes has been formed and then it increased the residue in the TG curve over the ILDHs contribution. These changes indicate that LDHs can catalyze the carbon double bonds to form stable char structure, such as aromatic structure. These results give further evidence that organic phosphorus in ILDHs/EP blend has been converted into phosphocarbonaceous complexes in char after oxidation.

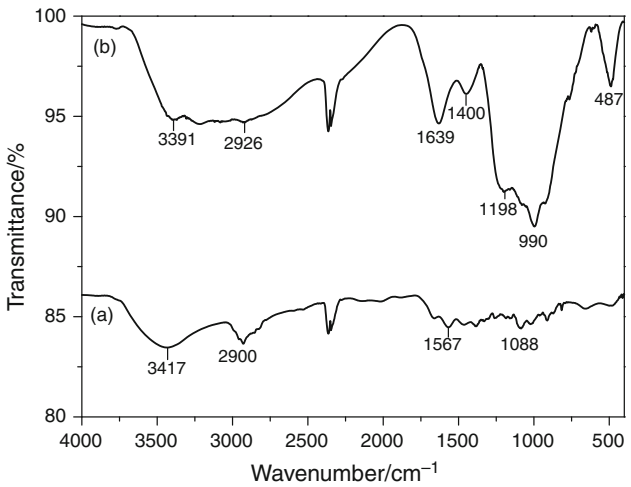

Fig. 9 FTIR spectra of residue: **a** EP and **b** ILDHs/EP-20

The effect of the char structure on the flame retardancy of EP matrix has been studied further. The morphologies of the charred layers obtained after LOI test were examined by SEM. As shown in Fig. 10a, the image of outer surface of ILDHs/EP-20 char seems fluffy and porous. The lamellar structure of LDHs can clearly be seen in Fig. 10a, b. The addition of ILDHs to epoxy folded the morphology of char. Both closed holes and opened holes are found in the char. This depends on the viscosity of ILDHs/EP-20 melted and release of composite. Generally, the closed hole is better than opened hole, because the closed hole can provide a good barrier in combing with the swollen inner structure (Fig. 10c) to the transfer of heat, mass and flammable gases during combustion which improved the flame retardancy of intumescent flame-retarded epoxy samples more efficiently [32].

Based on the analysis aforementioned, a possible mechanism for the ILDHs/EP-20 composites was discussed. During combustion, AAPP is first thermally decomposed to form phosphorylated polyvinyl alcohol which may undergo a further dehydration in two traditional ways. The phosphate ester may react with the EP network or itself and subsequently cross-link with the formation of a three-dimensional network structure. Then, phosphorylated polyvinyl alcohol may react with the LDHs layers and release water molecules to produce bridges between AAPP chains. Wang et al. [33] reported that only 1.5 % nano-LDHs could catalyze the esterification reaction between ammonium polyphosphate and pentaerythritol. The formation of a small number of such bridges will induce a stabilization of AAPP and a decrease in the volatility of phosphorus, and thus, more AAPP will be available for phosphorylation and char formation [34]. So, the viscosity

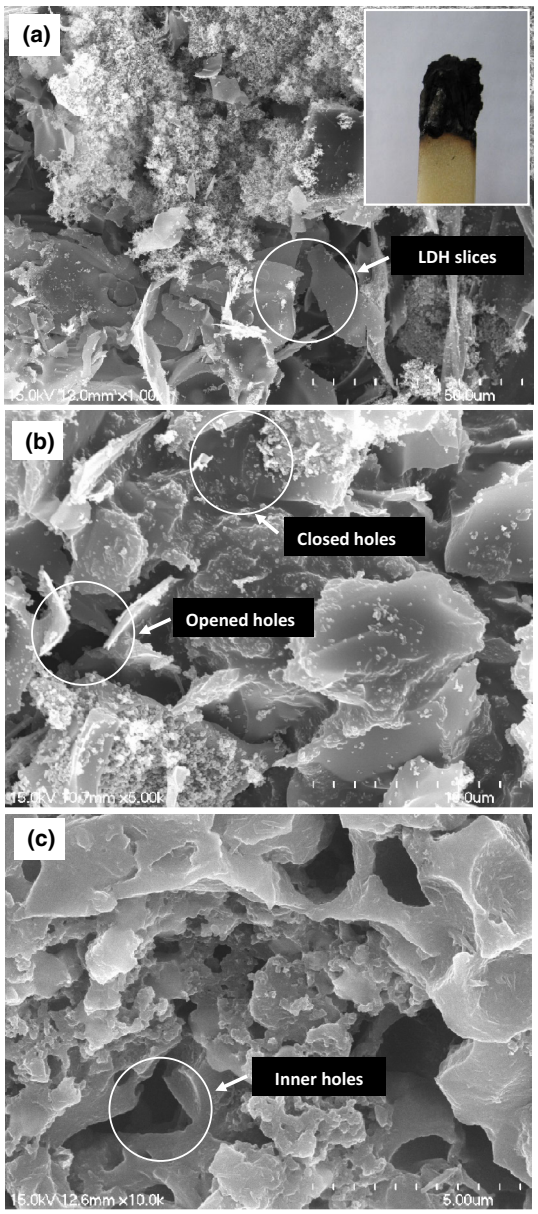

Fig. 10 SEM images of ILDHs/EP-20 residue with **a** ×1000, **b** ×5000 and **c** ×10,000 magnifications. The *inset* shows the morphology of residue

of the melt during pyrolysis and combustion increases and therefore enhances the formation of a compact and dense charred layer. There is also an intumescent char structure which is produced by releasing H_2O and NH_3. Simultaneously, during the combustion, the reaction of EP chains with LDHs results in a precursor of char. As described above, the improvement in flammability properties of the ILDHs/EP-20 composite is mainly attributed to the condensed-phase flame-retarding mechanism. The reinforced char layers during combustion led to a production of low volatiles [35]. Meanwhile, there also exists a minor gas-phase flame-retarding mechanism. The LDHs can promote the formation of a compact charred layer in the condensed phase during combustion. Furthermore, the intumescent char structure prevents the internal thermal decomposition products from getting out into the flame zone and the O_2 from getting into the polymer matrix [6].

Conclusions

To enhance the flammability and mechanical properties of epoxy/LDHs composites, an ammonium alcohol polyvinyl phosphate (AAPP) intercalated LDHs (ILDHs) were synthesized by a solution intercalation method. The conditions for synthesis of ILDHs have been optimized. As the AAPP-to-LDHs were 1:2, the reaction time was 2 h, the reaction temperature was 90 °C, and the yield of ILDHs was about 73.6 %. The flame retardancy of epoxy was improved by adding ILDHs. The ILDHs/EP containing 30–40 mass% ILDHs passed UL-94 V-0 rating. Tensile strength was also enhanced by adding 10–20 mass% ILDHs, which was attributed to the involvement of physical cross-linking network among layered particles and polymer chains. SEM observations of the residues of ILDHs/EP confirmed the formation of an incompact charred layer during combustion, which could inhibit the transmission of heat and mass during contact with flame. Analysis revealed both condensed-phase and gas-phase flame-retarding mechanisms for ILDHs/EP, in which ILDHs acted as a catalyst for esterification, dehydration and compact char formation of EP system.

Acknowledgements The authors thank the Priority Academic Program Development of Jiangsu (China) Higher Education Institutions (JHB2012-48) and Jiangsu Key Laboratory for Environment Functional Materials (SJHG1306) for financial support.

References

1. Lu H, Song L, Hu Y. A review on flame retardant technology in China. Part II: flame retardant polymeric nanocomposites and coatings. Polym Adv Technol. 2011;22:379–94.
2. Tsai T-Y, Lu S-W, Li F-S. Preparation and characterization of epoxy/layered double hydroxides nanocomposites. J Phys Chem Solids. 2008;69(5–6):1386–90.
3. Zhao Y, Li F, Evans DG, Duan X. Smoke suppression effects of LDHs nanomaterials for epoxy resin. Chin J Appl Chem. 2002;19:954–7.
4. Becker CM, Gabbardo AD, Wypych F, Amico SC. Mechanical and flame-retardant properties of epoxy/Mg–Al LDHs composites. Appl Sci Manuf. 2011;42:196–202.
5. Becker CM, Dick TA, Ramos JT, Wypych F, Amico SC. The effect of the addition of Mg–Al LDHs intercalated with dodecyl sulfate on the fire retardancy properties of epoxy. Macromol Symp. 2012;319:129–35.

6. Becker CM, Dick TA, Wypych F, Schrekker HS, Amico SC. Synergetic effect of LDHs and glass fiber on the properties of two- and three-component epoxy composites. Polym Test. 2012;31:741–7.
7. Chan Y-N, Juang T-Y, Liao Y-L, Dai SA, Lin J-J. Preparation of clay/epoxy nanocomposites by layered-double-hydroxide initiated self-polymerization. Polymer. 2008;49:4796–801.
8. Tseng C-H, Hsueh H-B, Chen C-Y. Effect of reactive layered double hydroxides on the thermal and mechanical properties of LDHs/epoxy nanocomposites. Compos Sci Technol. 2007;67: 2350–62.
9. Hsueh H-B, Chen C-Y. Preparation and properties of LDHs/epoxy nanocomposites. Polymer. 2003;44:5275–83.
10. Ramaraj B, Jaisankar SN. Thermal and morphological properties of poly (vinyl alcohol) and layered double hydroxide (LDHs) nanocomposites. Polym Plast Technol Eng. 2008;47:733–8.
11. Ramaraj B, Nayak SK, Yoon KR. Poly (vinyl alcohol) and layered double hydroxide composites: thermal and mechanical properties. J Appl Polym Sci. 2010;116:1671–7.
12. Li BG, Hu Y, Zhang R, Chen ZY, Fan WC. Preparation of the poly (vinyl alcohol)/layered double hydroxide nanocomposite. Mater Res Bull. 2003;38:1567–72.
13. Huang GB, Fei ZD, Chen XY, Qiu FL, Wang X, Gao JR. Functionalization of layered double hydroxides by intumescent flame retardant: preparation, characterization, and application in ethylene vinyl acetate copolymer. Appl Surf Sci. 2012;258: 10115–22.
14. Zhao C-X, Liu Y, Wang D-Y, Wang D-L, Wang YZ. Synergistic effect of ammonium polyphosphate and layered double hydroxide on flame retardant properties of poly (vinyl alcohol). Polym Degrad Stab. 2008;93:1323–31.
15. Liu XC, Chen J, Zou J, Duan HZ, Li JD, Chen CX, Meng PR. Preparation and membrane separation performances of quarternized ammonium cationic polyvinyl alcohol. J Appl Polym Sci. 2011;119:2584–94.
16. Kameda T, Tsuchiya Y, Yamazaki T, Yoshioka T. Preparation of Mg–Al layered double hydroxides intercalated with alkyl sulfates and investigation of their capacity to take up *N*,*N*-dimethylaniline from aqueous solutions. Solid State Sci. 2009;11:2060–4.
17. Klemkaite K, Prosycevas I, Taraskevicius R, Khinsky A, Kareiva A. Synthesis and characterization of layered double hydroxides with different cations (Mg, Co, Ni, Al), decomposition and reformation of mixed metal oxides to layered structures. Cent Eur J Chem. 2011;9:275–82.
18. Langford JI, Wilson AJC. Scherrer after sixty years: a survey and some new results in the determination of crystallite size. J Appl Cryst. 1978;11:102–13.
19. Fleutot S, Dupin J-C, Renaudin G, Martinez H. Intercalation and grafting of benzene derivatives into zinc-aluminum and copper-chromium layered double hydroxide hosts: an XPS monitoring study. Phys Chem Chem Phys. 2011;13:17564–78.
20. Gu Z, Wu A, Li L, Xu ZP. Influence of hydrothermal treatment on physicochemical properties and drug release of anti-inflammatory drugs of intercalated layered double hydroxide nanoparticles. Pharmaceutics. 2014;6:235–48.
21. Qin J, Xie P, Tian Y, Zhang H, Yu J. Preparation and characterisation of ammonium polyphosphate intercalated layered double hydroxides composite by joint method with or without sonochemical technique. J Therm Anal Calorim. 2012;110:1193–8.
22. Chen W, Qu B. Enhanced thermal and mechanical properties of poly (methyl acrylate)/ZnAl layered double hydroxide nanocomposites formed by in situ polymerization. Polym Deg Stab. 2005;90:162–6.
23. Qin HL, Zhang SM, Zhao CG, Hu GJ, Yang MS. Flame retardant mechanism of polymer/clay nanocomposites based on polypropylene. Polymer. 2005;46:8386–95.
24. Qiu LZ, Chen W, Qu BJ. Morphology and thermal stabilization mechanism of LLDPE/MMT and LLDPE/LDHs nanocomposites. Polymer. 2006;47:922–30.
25. Pérez-Ramírez J, Mul G, Kapteijn F, Moulijn JA. In situ investigation during the thermal decomposition of Co–Al-HTlc in different atmospheres. J Mater Chem. 2001;11:821–30.
26. Wang Z, Han E, Ke W. Effect of nanoparticles on the improvement in fire-resistant and anti-ageing properties of flame-retardant coating. Surf Coat Tech. 2006;200:5706–16.
27. Bashar M, Sundararaj U, Mertiny P. Microstructure and mechanical properties of epoxy hybrid nanocomposites modified with acrylic tri-block-copolymer and layered-silicate nanoclay. Compos Part A Appl Sci Manuf. 2012;43:945–54.
28. Lin YJ, Li DQ, Evans DG, Duan X. Modulating effect of Mg/Al-CO_3 layered double hydroxides on the thermal stability of PVC resin. Polym Degrad Stab. 2005;88:286–93.
29. Song RJ, Zhang BY, Huang BT, Tang T. Synergistic effect of supported nickel catalyst with intumescent flame-retardants on flame retardancy and thermal stability of polypropylene. J Appl Polym Sci. 2006;102:5988–93.
30. Guo J, He M, Li Q, Yu J, Qin S. Synergistic effect of organo-montmorillonite on intumescent flame retardant ethylene–octene copolymer. J Appl Polym Sci. 2013;129:2063–9.
31. Du B, Guo Z, Fang Z. Effects of organo-clay and sodium dodecyl sulfonate intercalated layered double hydroxide on thermal and flame behaviour of intumescent flame retarded polypropylene. Polym Degrad Stab. 2009;94:1979–85.
32. Wang Z, Han E, Ke W. Influence of nano-LDHs on char formation and fire-resistant properties of flame-retardant coating. Prog Organ Coat. 2005;53:29–37.
33. Zhang Z, Bin L, Mei X, Xu C. Study on fire retardant mechanism of nano-LDHs in intumescent system. Sci China B Chem. 2007;50:392–6.
34. Lewin M. Synergism and catalysis in flame retardancy of polymers. Polym Adv Technol. 2001;12:215–22.
35. Wang D-Y, Das A, Leuteritz A, Mahaling RN, Jehnichen D, Wagenknecht U, Heinrich G. Structural characteristics and flammability of fire retarding EPDM/layered double hydroxide (LDHs) nanocomposites. RSC Adv. 2012;2:3927–33.